

# Analytical Methods

Accepted Manuscript



This is an *Accepted Manuscript*, which has been through the Royal Society of Chemistry peer review process and has been accepted for publication.

*Accepted Manuscripts* are published online shortly after acceptance, before technical editing, formatting and proof reading. Using this free service, authors can make their results available to the community, in citable form, before we publish the edited article. We will replace this *Accepted Manuscript* with the edited and formatted *Advance Article* as soon as it is available.

You can find more information about *Accepted Manuscripts* in the [Information for Authors](#).

Please note that technical editing may introduce minor changes to the text and/or graphics, which may alter content. The journal's standard [Terms & Conditions](#) and the [Ethical guidelines](#) still apply. In no event shall the Royal Society of Chemistry be held responsible for any errors or omissions in this *Accepted Manuscript* or any consequences arising from the use of any information it contains.

1  
2  
3  
4                   **Synthesis and characterization of a magnetic molecularly imprinted**  
5  
6                   **polymer for the selective extraction of nicotine and cotinine from urine**  
7  
8                   **samples followed by GC-MS analysis**  
9  
10

11  
12  
13  
14  
15  
16  
17  
18  
19  
20                   Lidiane Silva Franqui<sup>a</sup>, Mariane Gonçalves Santos<sup>a</sup>, Luciano Sindra Virtuoso<sup>b</sup>, Patrícia Penido  
21                   Maia<sup>a</sup>, Eduardo Costa Figueiredo<sup>a\*</sup>  
22  
23

24  
25                   <sup>a</sup>Toxicants and Drugs Analysis Laboratory, Faculty of Pharmaceutical Sciences, Federal  
26                   University of Alfenas - Unifal-MG, 700 Gabriel Monteiro da Silva street, 37130-000, Alfenas,  
27                   MG, Brazil  
28  
29

30                   <sup>b</sup>Colloid Chemistry Group, Chemistry Institute, Federal University of Alfenas - Unifal-MG, 700  
31                   Gabriel Monteiro da Silva street, 37130-000, Alfenas, MG, Brazil  
32  
33

34  
35                   \*Corresponding author: Tel.: +55 35 3299 1342; Fax: +55 35 3299 1067  
36

37                   E-mail: eduardocfig@yahoo.com.br  
38  
39  
40  
41  
42  
43  
44  
45  
46  
47  
48  
49  
50  
51  
52  
53  
54  
55  
56  
57  
58  
59  
60

**Abstract**

A magnetic molecularly imprinted polymer (MMIP) was synthesized, characterized and used in the selective extraction of nicotine and cotinine from urine samples, followed by GC-MS analysis. Fe<sub>3</sub>O<sub>4</sub> nanoparticles were prepared by the co-precipitation method, silanized/stabilized with tetraethyl orthosilicate and functionalized with 3-(trimethoxysilyl) propyl methacrylate. The MMIP was prepared on the magnetic nanoparticle surface, using nicotine as the template and methacrylic acid as the functional monomer. The material was characterized by scanning electron microscopy, atomic force microscopy, Fourier transform infrared spectroscopy, energy dispersive X-ray spectrometry and thermogravimetry, where all the synthesis steps were confirmed. The nanoparticles were used in the dispersive solid phase extraction of nicotine and cotinine from human urine samples, and the extracts were analyzed by GC-MS. The analytical curves ranged from 0.1 to 3.0 mg L<sup>-1</sup> ( $r > 0.99$ ), with a limit of quantification (LOQ) of 0.1 mg L<sup>-1</sup> for both analytes. The intra and inter-day precisions were less than 20% for the LOQ and less than 15% for the other points; whereas the intra and inter-day accuracies were within  $\pm 9\%$ . The method was successfully employed to analyze nicotine and cotinine from four real smokers' urine samples.

**Keywords:** Magnetic molecular imprinted polymers; Molecular recognition; Magnetic susceptibility; GC-MS; Nicotine; Cotinine.

## Introduction

Currently, analytical chemistry is in a very advanced stage in terms of sophisticated equipment availability, for substance separation, identification and quantification. However, despite these advances, in some cases, direct analysis is not possible, because most of the samples have complex matrices with a large number of interferents, which can compromise the precision and accuracy of the used methods, as well as harm the equipments. Thus, the sample preparation stage is critical in order to obtain reliable results and has received great attention recently.<sup>1</sup>

The need to analyze complex samples on a large scale stimulates the exploration of faster, simpler and more selective sample preparation methods.<sup>2</sup> and this led to a great evolution in the development of new selective techniques, such as those based on the use of molecularly imprinted polymers (MIPs).<sup>3</sup>

The MIPs are synthetic polymeric materials that have specific cavities for a target molecule, involving a retention mechanism based on molecular recognition. Besides the possibility to prepare sorbents with predetermined selectivity<sup>4</sup>, MIPs have additional advantages such as easiness and low cost of the synthesis, chemical, physical and thermal stabilities and the possibility to be used for a wide range of target molecules. Thus, polymers have been widely used in analytical techniques, mainly as selective sorbents in solid phase extraction (SPE).<sup>3,5</sup>

Despite the advantages of the conventional molecularly imprinted solid phase extraction (MISPE) in cartridges, some drawbacks of this technique can be emphasized, such as its poor mass transfer, low binding capacity and slow binding kinetics.<sup>6</sup> Hence, a new modality of MIP, denominated magnetic molecularly imprinted polymer (MMIP)<sup>7</sup>, has received great attention in order to overcome these drawbacks. MMIPs are magnetic nanoparticles covered with MIP, resulting in a magnetically susceptible selective material. This sorbent can be added directly into the sample, being afterwards recovered by an external magnet. The obstruction of conventional SPE cartridges, caused by the sample matrix, is avoided,<sup>7,8</sup> and the pretreatment time is reduced, because of the exposed bigger surface area, improving the binding kinetics and capacity. For example, a sensitive method based on MMIP was developed by Chen *et al.*<sup>9</sup> to extract tetracycline antibiotics from tissue and egg samples. When compared with the molecularly imprinted solid phase

1  
2  
3  
4 microextraction method (MIP-SPME)<sup>10</sup>, the MMIP provided lower limit of detection (LOD)  
5 and higher precision (LOD 0.06-0.19 ng.g<sup>-1</sup> and RSD 3.4-5.8% for MMIP; LOD 1.5-3.5 ng.g<sup>-1</sup>  
6 and RSD 2.9-12.3% for MIP-SPME). Moreover, the molecularly imprinted solid phase  
7 extraction method (MIP-SPE)<sup>11</sup> presented extraction recoveries of about 69%, whereas in the  
8 MMIP method the recoveries were >93%. In another study, Zhang *et al.*<sup>12</sup> synthesized a  
9 MMIP to extract sterols from complicated biological samples. With this MMIP, they obtained  
10 LOD values about 1.2 and 1.1 µg L<sup>-1</sup> for stigmasterol and β-sitosterol from serum samples,  
11 respectively, which are lower than 17 and 31 µg L<sup>-1</sup> obtained by conventional solid phase  
12 extraction (SPE)<sup>13</sup>, and than 7.5 and 13 ng mL<sup>-1</sup> obtained by online SPE<sup>14</sup>, for the same  
13 analytes and samples. Additionally, MMIPs have been used to extract several analytes from  
14 different samples like herbal medicines,<sup>15-17</sup> water,<sup>18-20</sup> urine,<sup>21,22</sup> fruit,<sup>12,23</sup> honey,<sup>24</sup> egg,<sup>25</sup>  
15 milk,<sup>26</sup> wine,<sup>27</sup> poultry feed,<sup>28</sup> serum,<sup>12</sup> mushroom,<sup>12</sup> soil,<sup>29</sup> soybean,<sup>29</sup> millet,<sup>29</sup> plant  
16 tissues<sup>30</sup>, pork and pig liver<sup>31</sup>.

17  
18  
19  
20  
21  
22  
23  
24  
25  
26  
27  
28 Nowadays, it is common knowledge that smoking is among the leading preventable  
29 causes of morbidity and mortality worldwide, being considered as the main cause of lung  
30 cancer and an important factor for cardiovascular and chronic pulmonary inflammatory  
31 diseases, among other conditions.<sup>32</sup> More than 4,000 compounds have been isolated and  
32 identified in tobacco smoke, of which more than 20 are alkaloids.<sup>33</sup> Nicotine is the most  
33 abundant pharmacologically active alkaloid in tobacco (98% of the total alkaloids) being  
34 responsible for its dependency. Furthermore, nicotine is a highly potent toxic agent<sup>34</sup>, with a  
35 primarily hepatic biotransformation and a half-life of about 2 h. The main product of nicotine  
36 biotransformation is cotinine, and because of its high half-life, it can be determined in  
37 different biological fluids, for several days after exposure to tobacco smoke.<sup>33, 35</sup> Thus,  
38 nicotine and cotinine have been widely used as biological markers to determine smoking  
39 habits.

40  
41  
42  
43  
44  
45  
46  
47  
48 Therefore, MMIPs show up as promising tools for the use in complex sample  
49 preparation techniques. In this sense, this study aimed to synthesize a MMIP for the  
50 extraction of nicotine and cotinine from urine for the purpose of monitoring exposure to  
51 tobacco smoke.  
52  
53  
54  
55  
56  
57  
58  
59  
60

## Experimental

### Chemicals and samples

HPLC grade methanol and acetonitrile were purchased from Sigma-Aldrich® (Steinheim, Germany). Nicotine and cotinine stock solutions (both from Sigma-Aldrich®, Steinheim, Germany) were prepared at a concentration of 1.0 mg mL<sup>-1</sup>, in HPLC grade methanol, placed in amber flasks and stored at -18 °C for up to 30 days. Ferric chloride (FeCl<sub>3</sub>·6H<sub>2</sub>O), ferrous chloride (FeCl<sub>2</sub>·4H<sub>2</sub>O), 3-(methacryloyl) propyl trimethoxysilane (MPS), tetraethyl orthosilicate (TEOS), methacrylic acid (MAA), ethylene glycol dimethacrylate (EGDMA), 4,4'-Azobis(4-cyanovaleric acid) (ABCVA) (all from Sigma-Aldrich®, Steinheim, Germany) were used in the MMIP synthesis. Sodium dihydrogen phosphate (NaH<sub>2</sub>PO<sub>4</sub>·H<sub>2</sub>O) and disodium hydrogen phosphate (Na<sub>2</sub>HPO<sub>4</sub>) were obtained from Cinética Química Ltda (São Paulo, Brazil) and Vetec® (Rio de Janeiro, Brazil), respectively. Ammonium hydroxide (28%, v/v) and 2-Propanol were both obtained from Isofar® (Rio de Janeiro, Brazil). Hydrochloric and acetic acids were purchased from Furlab® (São Paulo, Brazil) and Êxodo Científica (São Paulo, Brazil), respectively.

Human urine sample handling was approved by the ethics committee of the Federal University of Alfenas (registration number 18026513.8.0000.5142). The methodology was developed using pool urine samples (n=5) obtained from volunteer non-smokers, aged between 20 to 50 years, in order to offset the matrix effect in the extraction process of the urine samples. For nicotine and cotinine determination, urine samples (n=4) were obtained from volunteers who reported being smokers, in the same age group. All samples were centrifuged during 10 min at 10,000 m s<sup>-2</sup>, and directly submitted to extraction by MMIP.

### Apparatus

The MMIP synthesis was performed using an ultrasonic bath (model USC2800A, Unique, São Paulo, Brazil), a heater plate (model NT103, Novatécnica, São Paulo, Brazil), a mechanical stirrer (model TE-099 Unidade Potter, Tecnal, São Paulo, Brazil), a double boiler (Frigomix B) coupled with thermostat (Thermomix BM) (B. Braun Biotech International, Melsungen, Germany), a tube shaker (Glas-Col, Washington, USA) and a vacuum drying oven

1  
2  
3  
4 (Novatécnica, São Paulo, Brazil). The extractions were processed with a tube shaker (Vibrax  
5 VXR basic, IKA, São Paulo, Brazil) and a ferromagnetic magnet. The chromatographic  
6 analyses were performed using a Shimadzu GC-2010 gas chromatograph coupled to a mass  
7 spectrometer (GC-MS) and an AOC 20i+s autoinjector (Shimadzu®, Kyoto, Japan). The MMP  
8 was characterized by Fourier transform infrared spectrometer - FT-IR (model IS50, Thermo  
9 Scientific, Waltham, USA), thermogravimetric analysis - TGA (model SDT Q600, TA  
10 Instruments, New Castle, USA), scanning electron microscopy/energy dispersive X-ray  
11 spectrometry - SEM/EDS (model LV-JSM 6360, JEOL, Tokyo, Japan) and atomic force  
12 microscopy - AFM (NanoScope IIIa, Veeco Instruments, New York, USA).  
13  
14  
15  
16  
17  
18  
19

#### 20 21 22 Synthesis of the MMIP 23

24  
25 The MMIP was synthesized in four steps. Initially, the Fe<sub>3</sub>O<sub>4</sub> nanoparticles were  
26 prepared by the coprecipitation method according to Chen *et al.*<sup>27</sup> Thus, 15 mmol of  
27 FeCl<sub>3</sub>·6H<sub>2</sub>O and 10 mmol of FeCl<sub>2</sub>·4H<sub>2</sub>O were dissolved in 80 mL of deionized water  
28 preheated to 80°C, under nitrogen gas and vigorous stirring. So, 50 mL of 28% (v/v)  
29 ammonium hydroxide solution was dropwise added into the solution that changed its color  
30 from clear yellow to black. The mixture was maintained in standby at 80 °C for 30 min. The  
31 obtained black precipitate (Fe<sub>3</sub>O<sub>4</sub> nanoparticles) was collected by an external magnet and  
32 washed repeatedly with deionized water until the used washing solution presented pH from  
33 6.5 to 7.5. Finally, the particles were dried under vacuum at 60 °C for 24 h.  
34  
35  
36  
37  
38  
39  
40

41 In the second step, the surface of Fe<sub>3</sub>O<sub>4</sub> nanoparticles was modified with SiO<sub>2</sub>  
42 according to a study by Zeng *et al.*<sup>16</sup>, resulting in Fe<sub>3</sub>O<sub>4</sub>@SiO<sub>2</sub>. Then, 600 mg of Fe<sub>3</sub>O<sub>4</sub>  
43 nanoparticles was added in 60 mL of isopropanol:ultra-pure water (5:1, v/v), and the  
44 suspension was maintained in the ultrasonic bath for 20 min. Afterwards, 10 mL of 28% (v/v)  
45 ammonium hydroxide solution and 4 mL of TEOS were added promptly, where the reaction  
46 was maintained at room temperature with continuous stirring for 12 h. Following this, the  
47 modified magnetic nanoparticles were separated by an external magnet, washed repeatedly  
48 with deionized water until the used washing solution presented pH from 6.5 to 7.5. Finally,  
49 the particles were dried under vacuum at 60 °C for 24 h.  
50  
51  
52  
53  
54  
55  
56

57 In the third step, the Fe<sub>3</sub>O<sub>4</sub>@SiO<sub>2</sub> particles were functionalized with polymerizable  
58 double bonds according to Kong *et al.*<sup>28</sup>, resulting in vinyl-modified Fe<sub>3</sub>O<sub>4</sub>@SiO<sub>2</sub>. Therefore,  
59  
60

1  
2  
3  
4 200 mg of  $\text{Fe}_3\text{O}_4@\text{SiO}_2$  was dispersed in 50 mL of methanol by sonication for 30 min. Then, 3  
5 mL of MPS was added drop by drop under vigorous stirring. The reaction was maintained for  
6 48 h at the room temperature and continuous stirring. The resultant product was collected  
7 by an external magnet, rinsed with methanol for several times until the supernatant became  
8 clearer then dried under vacuum at 60 °C for 24 h.  
9

10  
11  
12  
13 In the last step, the MIP was synthesized (by the precipitation polymerization method)  
14 over the vinyl-modified  $\text{Fe}_3\text{O}_4@\text{SiO}_2$ , resulting in the MMIPs. Thus, 0.4 mmol of nicotine  
15 (template) and 2.0 mmol of MAA (functional monomer) were dissolved in 20 mL of  
16 acetonitrile, while 489 mg of vinyl-modified  $\text{Fe}_3\text{O}_4@\text{SiO}_2$  nanoparticles was added into  
17 another flask containing 20 mL of acetonitrile. Then, both flasks were placed simultaneously  
18 in the ultrasonic bath for 1h to form the template-monomer complex and magnetic  
19 nanoparticles dispersion, respectively. Subsequently, the template-monomer complex was  
20 poured into the magnetic nanoparticle dispersion, and 12.0 mmol of EGDMA (cross-linker)  
21 and 80 mg of ABCVA (initiator) were immediately added into the mixture under vigorous  
22 stirring. The mixture was degassed in an ultrasonic bath for 30 min and bubbled with  
23 nitrogen gas for 15 min to remove the oxygen. The flask was sealed and the polymerization  
24 was performed at 75 °C under mechanical stirring for 24 h. The MMIPs were collected  
25 magnetically, washed sequentially with methanol:acetic acid solution (9:1, v/v) and pure  
26 methanol to remove the template and other reagents remaining from the synthesis. Finally,  
27 the particles were dried under vacuum at 60 °C for 24 h.  
28  
29  
30  
31  
32  
33  
34  
35  
36  
37  
38  
39  
40

#### 41 Characterization

42  
43  
44  
45 The morphology of the materials was investigated using SEM and AFM. The  
46 encapsulation efficiency of the microspheres was measured by FT-IR, EDS and TGA.

47  
48 The infrared spectra was recorded on a FT-IR spectrometer performed in attenuated  
49 total reflectance (ATR) mode in a wavelength range of 4000-400  $\text{cm}^{-1}$ . TGA was performed  
50 starting from room temperature to 800 °C, with a heating rate of 10 °C  $\text{min}^{-1}$  and with a  
51 nitrogen flow of 100 mL  $\text{min}^{-1}$ . For SEM/EDS analyses, the samples were previously coated  
52 with a thin layer of platinum and the microscopy operated at an acceleration voltage of 15  
53 kV. For AFM analyses, sample dispersion droplets were dried on top of freshly cleaved mica  
54 surfaces and glued to the instrument sample holder. The analyses were carried out  
55  
56  
57  
58  
59  
60



1  
2  
3  
4 employing a magnetic tip (silicon coated with cobalt), a resonance frequency of 75 kHz and a  
5 constant pressure of  $2.8 \text{ N m}^{-1}$ .  
6  
7

#### 8 9 Extraction procedure

10  
11  
12 Twenty milligrams of MMIP was added into a test tube containing 2.0 mL of a urine  
13 sample. The tube was vortexed during 20 min. Then, the MMIP particles were separated by  
14 an external magnet and the urine sample was discarded. Therefore, the analytes were  
15 eluted from the MMIP using a mixture of 3.0 mL of pure methanol and 25  $\mu\text{L}$  of  $0.1 \text{ mol L}^{-1}$   
16 HCl aqueous solution, stirring vigorously for 20 min. Afterwards, 2.7 mL of the supernatant  
17 was transferred into another test tube, and evaporated to dryness under vacuum at  $60^\circ\text{C}$ .  
18 Finally, the residues were dissolved in 200  $\mu\text{L}$  of pure methanol and analyzed by GC-MS.  
19  
20  
21  
22  
23  
24  
25  
26

#### 27 Chromatographic conditions

28  
29  
30 Nicotine and cotinine were analyzed by GC-MS, using a RTX5-MS column (30 m x 0.25  
31 mm i.d.; 0.25  $\mu\text{m}$  film thickness) with helium as the carrier gas at a flow rate of  $1.6 \text{ mL min}^{-1}$ .  
32 Two microliters was injected in the splitless mode, at  $250^\circ\text{C}$  (injector temperature). The  
33 oven temperature was programmed from 120 to  $280^\circ\text{C}$  at  $40^\circ\text{C min}^{-1}$ , and maintained at  
34  $280^\circ\text{C}$  for 4 min. The interface temperature was set at  $280^\circ\text{C}$  and the ion source was  
35 operated in the electron ionization mode (EI; 70 eV,  $250^\circ\text{C}$ ). Full-scan mass spectra ( $m/z$   
36 from 40 to 200) was recorded for both analyte identifications. Selective ion monitoring (SIM)  
37 mode was used in the quantitative analyses. The ions at  $m/z$  162, 84, 133 and  $m/z$  176, 147,  
38 98 were used to monitor nicotine and cotinine, respectively. The quantification was based  
39 on the peak area integration at  $m/z$  84 and 98 for nicotine and cotinine, respectively. The  
40 other ions served as qualifying ions. The total separation time was 8.0 min.  
41  
42  
43  
44  
45  
46  
47  
48  
49  
50

#### 51 Validation

52  
53  
54  
55 The linearity study was performed by analyzing the urine samples ( $n=5$ ) fortified with  
56 standard solutions of nicotine and cotinine at concentrations of 0.1, 0.5, 1.0, 2.0 and 3.0 mg  
57  $\text{L}^{-1}$ . The limits of quantification (LOQ) were defined as the lowest concentrations that can be  
58  
59  
60

1  
2  
3  
4 analyzed with precision and accuracy. The intra and inter-day precisions as well as accuracies  
5 were assessed using a blank urine sample (n=5) fortified with both nicotine and cotinine at  
6 0.1, 1.0 and 3.0 mg L<sup>-1</sup> concentrations. The recoveries were obtained by comparing the  
7 analytical signals of the extracted samples with the analytical signals of mixed nicotine and  
8 cotinine standard solutions, analyzed without extractions.  
9  
10  
11  
12

## 13 14 15 **Results and discussion**

### 16 17 18 Preparation of MMIPs

19  
20  
21  
22 At first, the Fe<sub>3</sub>O<sub>4</sub> nanoparticles were synthesized by the co-precipitation method for  
23 being the classical procedure for obtaining Fe<sub>3</sub>O<sub>4</sub> magnetic nanoparticles, due to its simplicity  
24 and higher efficiency in terms of yield and less reaction time.<sup>36</sup> According to Laurent, *et al.*<sup>36</sup>,  
25 a high concentration of iron salts used during the Fe<sub>3</sub>O<sub>4</sub> synthesis can favor the nucleation  
26 stage of the nanoparticles, resulting in a more homogeneous particle size distribution.  
27 Furthermore, magnetite (Fe<sub>3</sub>O<sub>4</sub>) is very unstable, being easily oxidized to maghemite  
28 (γ-Fe<sub>2</sub>O<sub>3</sub>) in the presence of oxygen and/or reacting with the excess of H<sup>+</sup> ions. Thus, the  
29 employment of an excess of ammonium hydroxide solution ensures a purer material  
30 production, with a minimal formation of maghemite.  
31  
32  
33  
34  
35  
36  
37

38 The surfaces of the Fe<sub>3</sub>O<sub>4</sub> nanoparticles were then coated with silica layers, reacting  
39 with TEOS. This procedure was carried out in order to prevent the oxidization and  
40 aggregation of the nanoparticles, as well as to provide them with superficial reactive silanol  
41 groups. Hence, the Fe<sub>3</sub>O<sub>4</sub>@SiO<sub>2</sub> superficial hydroxyl groups reacted with MPS to introduce  
42 vinyl groups on the surface of the nanoparticles, forming polymerizable sites. The double  
43 bonds on the surface of vinyl-modified Fe<sub>3</sub>O<sub>4</sub>@SiO<sub>2</sub> nanoparticles can react with  
44 methacrylate groups to initiate the co-polymerization of the MAA and EGDMA.  
45  
46  
47  
48  
49

50 The MIP synthesis was carried out according to Figueiredo *et al.*<sup>37</sup>, adopting the  
51 precipitation polymerization method followed by Chen *et al.*<sup>27</sup> Then, the MAA and EGDMA  
52 were chosen, respectively, as the functional monomer and cross-linker, as in Figueiredo's  
53 work. A racemic mixture of nicotine was used as the template molecule, since smokers are  
54 exposed to both enantiomers of nicotine, due to pyrolytic racemization of the S(-)-isomer  
55 during smoking<sup>38</sup>. In this way, the synthesized MIP is endowed with selective sites for both  
56  
57  
58  
59  
60

1  
2  
3  
4 enantiomeric forms of nicotine. According to literature, the functional monomer should be  
5 employed in a higher amount in relation to the template molecule in order to displace the  
6 equilibrium towards the formation of the template-monomer complex<sup>39</sup>. Furthermore, the  
7 cross-linker should be present in excess over the functional monomer to provide greater  
8 mechanical stability and appropriate porosity to the polymer<sup>6</sup>. So, an optimum molar ratio  
9 of 1:5:30 (template:MAA:EGDMA) was employed according to the results obtained by Chen  
10 *et al.*<sup>27</sup>

11  
12 The MMIP was used to extract nicotine and cotinine directly from untreated urine  
13 samples, which normally present pHs within 5.0 and 7.0. In this pH range, the pyrrolidinic  
14 (pka = 8.2) and pyridine (pka = 3.1) rings were positively ionized and non-ionized,  
15 respectively, whereas the carboxyl group (pka = 4.7) of the MAA was negatively ionized.  
16 Thus, the binding mechanism of the MMIP was based on the electrostatic interaction  
17 between the pyrrolidinic groups of nicotine/cotinine with the carboxyl group of the MAA.<sup>37</sup>

## 28 29 Characterization

30  
31  
32 The morphologies of Fe<sub>3</sub>O<sub>4</sub>, Fe<sub>3</sub>O<sub>4</sub>@SiO<sub>2</sub>, vinyl-modified Fe<sub>3</sub>O<sub>4</sub>@SiO<sub>2</sub> and MMIP were  
33 investigated by SEM (Fig. 1). It was not possible to observe the shape of the Fe<sub>3</sub>O<sub>4</sub>  
34 nanoparticles, probably due to the particle aggregations as well as the low-resolution of the  
35 micrographs (Fig. 1a). However, it can be clearly seen that Fe<sub>3</sub>O<sub>4</sub>@SiO<sub>2</sub> and vinyl-modified  
36 Fe<sub>3</sub>O<sub>4</sub>@SiO<sub>2</sub> are regular spheres (Fig. 1b and c, respectively), with particle sizes ranging from  
37 a few nanometers to about 1 μm. Despite having a low resolution, the MMIP micrograph  
38 (Fig. 1d) indicated that these particles are also spherical and aggregated as cluster forms.

39  
40 The Fe<sub>3</sub>O<sub>4</sub> and Fe<sub>3</sub>O<sub>4</sub>@SiO<sub>2</sub> nanoparticles were isolated and analyzed by topography  
41 and magnetic force microscopy (Fig. 2). The larger diameter of Fe<sub>3</sub>O<sub>4</sub>@SiO<sub>2</sub> is probably due  
42 to the presence of the TEOS layer. The magnetic force intensity is low and homogeneously  
43 distributed throughout the Fe<sub>2</sub>O<sub>3</sub> nanoparticle, probably due to its reduced size. However, a  
44 more intense magnetic force (clear color) could be observed in the core of the Fe<sub>3</sub>O<sub>4</sub>@SiO<sub>2</sub>  
45 nanoparticles (Fig. 2d) compared to its edges (dark color). This result can be explained by the  
46 fact that the magnetic tip is sensitive to the magnetic and electrical fields. Thus, in the core  
47 there is an association between the magnetic force of the Fe<sub>2</sub>O<sub>3</sub> nanoparticles with the  
48  
49  
50  
51  
52  
53  
54  
55  
56  
57  
58  
59  
60

1  
2  
3  
4 electrical forces of the chemical groups of the TEOS, whereas in the edges there is only the  
5 electrical force.  
6

7  
8 In the FT-IR spectra, the absorption band at about  $580\text{ cm}^{-1}$  was characteristic to the  
9 Fe-O vibration (Fig. 3a). The bands at  $800$ ,  $950$  and  $1070\text{ cm}^{-1}$  in  $\text{Fe}_3\text{O}_4@/\text{SiO}_2$  and vinyl-  
10 modified  $\text{Fe}_3\text{O}_4@/\text{SiO}_2$  FT-IR spectra (Fig. 3b and c, respectively) were attributed to the  
11 stretching of Si-O, Si-O-H and Si-O-Si, respectively, confirming that the  $\text{Fe}_3\text{O}_4$  nanoparticles  
12 were adequately coated with TEOS and MPS. The MMIPs displayed strong absorption band  
13 at about  $1735\text{ cm}^{-1}$  (characteristic of the ester C=O vibration) and less intense absorption  
14 bands at  $1386$  and  $1251\text{ cm}^{-1}$  (characteristic of the ester C-O vibration) attributed to  
15 EGDMA. Moreover, the bands at  $2924$  and  $2852\text{ cm}^{-1}$  corresponded to the symmetrical and  
16 asymmetrical stretching of  $\text{sp}^3$  carbon C-H bond. They also confirmed the presence of the  
17 polymeric layer on the magnetic nanoparticle surfaces.  
18  
19

20  
21 TGA was performed to attest the encapsulation efficiency of the magnetic  
22 nanoparticles as well as to establish the thermal stability of the materials. According to Fig.  
23 4, the lesser weight loss, in all the samples, at temperatures less than  $200^\circ\text{C}$  was attributed  
24 to water evaporation. A minimal weight loss (about 4.5%) was observed for the  $\text{Fe}_3\text{O}_4$   
25 nanoparticles heated to  $800^\circ\text{C}$  due to their inorganic nature. Besides water loss, the  
26  $\text{Fe}_3\text{O}_4@/\text{SiO}_2$  and vinyl-modified  $\text{Fe}_3\text{O}_4@/\text{SiO}_2$  nanoparticles demonstrated a weight loss of  
27 about 2.86 and 3.15%, respectively, when heated from  $200$  to  $800^\circ\text{C}$ . In the case of the  
28  $\text{Fe}_3\text{O}_4@/\text{SiO}_2$  nanoparticles, this result may be due to the hydroxyl group condensations  
29 and/or residual ethoxide group degradations, while for vinyl-modified  $\text{Fe}_3\text{O}_4@/\text{SiO}_2$  this  
30 weight loss probably was a result of the grafted MPS decomposition. Finally, the MMIP  
31 showed a greater weight loss (about 70.94%) compared to the other materials, which  
32 ensured the presence of an organic network.  
33  
34  
35  
36  
37  
38  
39  
40  
41  
42  
43  
44  
45

46  
47 Table 1 shows the chemical composition obtained by EDS for all the materials. The  
48 small amount of platinum in all samples is due to the platinum coating required to perform  
49 the analyses. For the  $\text{Fe}_3\text{O}_4$  nanoparticles, the presence of iron and oxygen atoms was  
50 observed in a large proportion as well as a small amount of carbon, which is probably due to  
51 some contamination. For the  $\text{Fe}_3\text{O}_4@/\text{SiO}_2$  nanoparticles, there was a reduction in the iron  
52 percentage and an increase in the oxygen percentage, besides a large amount of silicon,  
53 which proves that they were coated with TEOS. Furthermore, it is important to note a  
54 considerable amount of carbon (41.62%) in the  $\text{Fe}_3\text{O}_4@/\text{SiO}_2$  nanoparticles, which can be  
55  
56  
57  
58  
59  
60

1  
2  
3  
4 attributed to the presence of residual ethoxide groups on the particle surface. Likewise, the  
5 functionalization with MPS can be confirmed by the high carbon percentage in the vinyl-  
6 modified Fe<sub>3</sub>O<sub>4</sub>@SiO<sub>2</sub> nanoparticles. Although MPS contains silicon and oxygen in its  
7 chemical structure, the percentage of these atoms decreased probably because there was  
8 an increase in the carbon percentage (which now represents more than 50% of the sample).  
9 Finally, the polymerization on the magnetic nanoparticle surfaces can be attested since  
10 there was an increase in the carbon percentage as well as a reduction in the other  
11 constituents (e.g. oxygen, silicon and iron) in the MMIP sample. It is noteworthy that the  
12 presence of copper and zinc in very small quantities comes from impurities.  
13  
14  
15  
16  
17  
18  
19  
20

#### 21 Figures of merit

22  
23  
24  
25 The mass spectra of nicotine and cotinine obtained by SCAN analysis are shown in Fig.  
26 5. The most intense peaks for nicotine were at m/z 84 (base peak), 133 and 162 (molecular  
27 peak), whereas for cotinine, they were at m/z 98 (base peak), 147 and 176 (molecular peak).  
28 Therefore, the runs were performed in the SIM mode in order to increase the method's  
29 sensitivity and selectivity. The SIM chromatogram of an extracted urine sample spiked with 3  
30 mg L<sup>-1</sup> of nicotine and cotinine is shown in Fig. 6. As it can be seen, the chromatogram  
31 contains few interferents, confirming the MMIP selectivity for the analytes. Furthermore, for  
32 the same concentration of the analytes, the MMIP extracted significantly more nicotine than  
33 cotinine (Figure 6). This confirms the selectivity of the MMIP since nicotine was used as the  
34 template molecule. As cotinine has a very similar structure to nicotine, it was also extracted  
35 but in a lower proportion. Additionally, it is important to point out that the MMIP synthesis  
36 was very similar (in terms of template, functional monomers and cross linker proportion) to  
37 the synthesis of a MIP selective to nicotine in our previous publication<sup>37</sup>, and it was possible  
38 to conclude that MIP was really more selective to nicotine, in comparison with cotinine,  
39 anabasine, nor nicotine, and caffeine.  
40  
41  
42  
43  
44  
45  
46  
47  
48  
49  
50  
51

52 The evaluated validation parameters were linearity, limit of quantification, precision  
53 and accuracy. For this purpose, we used a urine pool obtained by mixing five samples from  
54 non-smokers, in order to offset the effect of the matrix in extraction processes of the urine  
55 samples. The method was linear for both analytes in the range from 0.1 to 3.0 mg L<sup>-1</sup>, with  
56 correlation coefficients larger than 0.99 (for both analytes). The regression equations were Y  
57  
58  
59  
60

1  
2  
3  
4 = 2,496,212X – 33,541 and Y = 551,186X + 8,556 for nicotine and cotinine, respectively,  
5  
6 where X was the concentration of the studied compounds and Y was the peak area. The limit  
7  
8 of quantitation (LOQ) for both analytes was 0.1 mg L<sup>-1</sup>. The intra and inter-day precision and  
9  
10 accuracy (Table 2) are in accordance with the FDA recommendations.<sup>40</sup> All the results  
11  
12 showed that the proposed method was sufficiently accurate, selective and simple for the  
13  
14 determination of nicotine and cotinine in human urine samples.

#### 15 16 17 Application to real samples

18  
19  
20 Under the optimized conditions, the proposed method was applied to analyze four  
21  
22 smokers' urine samples (in triplicate). Nicotine was detected in all the samples, but in  
23  
24 concentrations lower than the LOQ, whereas cotinine concentrations ranged from 0.191 to  
25  
26 0.276 mg L<sup>-1</sup>. These results can be explained by the short half-life of nicotine (about 2 h<sup>33</sup>),  
27  
28 and by the fact that the urine samples were collected in the morning. Thus, as already  
29  
30 preconized by the literature<sup>41</sup>, nicotine was not a suitable biomarker. On the other hand,  
31  
32 the proposed method was suitable for monitoring exposure to tobacco, since cotinine is the  
33  
34 most used biomarker for tobacco exposure, having a long half-life of about 20h and being  
35  
36 excreted in greater amounts in the urine. Furthermore, 0.1 mg L<sup>-1</sup> urinary cotinine is known  
37  
38 as a cut-off for active smokers.<sup>42</sup>

#### 39 40 Conclusions

41  
42  
43 In this study, a MMIP for nicotine and cotinine extraction from urine samples was  
44  
45 successfully prepared and characterized. The obtained MMIP was easily collected using an  
46  
47 external magnetic field, without any additional centrifugation or filtration step, avoiding the  
48  
49 use of packed columns/cartridges, like in the conventional SPE. The extraction procedure  
50  
51 was fast, simple and efficient. The MMIP was adequately used to extract nicotine and  
52  
53 cotinine directly from human real urine samples followed by GC-MS analyses, where some  
54  
55 advantages can be emphasized, like the good selectivity, sensitivity, reproducibility and  
56  
57 analytical frequency. Thus, we believe that the method can be easily applied in monitoring  
58  
59 tobacco exposure.  
60

## Acknowledgments

We thank the “**Fundação de Amparo à Pesquisa do Estado de Minas Gerais**” (FAPEMIG, Belo Horizonte, Brazil), Project CDS-APQ-01612-10, “**Conselho Nacional de Desenvolvimento Científico e Tecnológico**” (CNPq, Brasília, Brazil), Project 483371/2012-2 and **Coordenação de Aperfeiçoamento de Pessoal Nível Superior** (CAPES) for their financial support. We also thank the National Center for Research in Energy and Materials (CNPEM) and Chemistry Institute of Unicamp for the AFM and SEM analyses, respectively.

1  
2  
3  
4  
5  
6  
7  
8  
9  
10  
11  
12  
13  
14  
15  
16  
17  
18  
19  
20  
21  
22  
23  
24  
25  
26  
27  
28  
29  
30  
31  
32  
33  
34  
35  
36  
37  
38  
39  
40  
41  
42  
43  
44  
45  
46  
47  
48  
49  
50  
51  
52  
53  
54  
55  
56  
57  
58  
59  
60

## References

- [1] J.D. Winefordner. John Wiley & Sons, Inc., *Hoboken*, New Jersey, 2003.
- [2] Y. Chen, Z. Guo, X. Wang and C. Qiu, *J. Chromatogr., A*, 2008, **1184**, 191-219.
- [3] C. He, Y. Long, J. Pan, K. Li and F. Liu, *J. Biochem. Biophys. Methods*, 2007, **70**, 133-150.
- [4] V. Pichon, *J. Chromatogr. A*, 2007, **1152**, 41-53.
- [5] L.I. Andersson, *J. Chromatogr. B*, **2000**, 745, 3-13.
- [6] D.A. Spivak, *Adv. Drug Delivery Rev.*, 2005, **57**, 1779-1794.
- [7] L. Chen and B. Li, *Anal. Methods*, 2012, **4**, 2613-2621.
- [8] E. Benito-Pena, S. Martins, G. Orellana and M.C. Moreno-Bondi, *Anal. Bioanal. Chem.*, 2009, **393**, 235-245.
- [9] L. Chen, J. Liu, Q. Zeng, H. Wang, A. Yu, H. Zhang and L. Ding, *J. Chromatogr. A*, 2009, **1216**, 3710–3719.
- [10] X. Hu, J. Pan, Y. Hu, Y. Huo and G. Li, *J. Chromatogr. A*, 2008, **1188**, 97–107.
- [11] E. Caro, R. M. Marc\_e, P. A. G. Cormack, D. C. Sherrington and F. Borrull, *Anal. Chim. Acta*, 2005, **552**, 81–86.
- [12] Z. Zhang, W. Tan, Y. Hu and G. Li, *J. Chromatogr. A*, 2011, 1218, 4275-4283.
- [13] I. Mendiara, C. Domeño and C. Nerín, *J. Sep. Sci.*, 2012, 35, 3308-3316.
- [14] I. Mendiara, K. Bentayeb, C. Nerín and C. Domeño, *Talanta*, 2015, 132, 690–697.
- [15] F-F. Chen, X-Y. Xie and Y-P Shi, *Talanta*, 2013, **115**, 482-489.
- [16] H. Zeng, Y.Z. Wang, C. Nie, J.H. Kong and X.J. Liu, *Analyst*, 2012, **137**, 2503-2512.
- [17] W, Li, L. Yang, F. Wang, H. Zhou, X. Yang, Y. Huang and H. Liu, *Biochem. Eng. J.*, 2013, **79**, 206-213.
- [18] S. Shi, J. Guo, Q. You, X. Chen and Y. Zhang, *Chem. Eng. J.*, 2014, **243**, 485-493.
- [19] Y. Hiratsuka, N. Funaya, H. Matsunaga and J. Haginaka, *J. Pharm. Biomed. Anal.*, 2013, **75**, 180-185.
- [20] Y-L. Zhang, J. Zhang, C-M Dai, X-F. Zhou and S-G. Liu, 2013, **97**, 809-816.



- 1  
2  
3  
4 [21] T. Jing, H. Xia, Q. Guan, W. Lu, Q. Dai, J. Niu, J-M. Lim, Q. Hao, Y-I. Lee, Y. Zhou and S.  
5 Mei, *Anal. Chim. Acta*, 2011, **692**, 73-79.  
6  
7  
8 [22] M. Bouri, M.J. L-García, R. Salghi, M. Zougagh and A. Ríos, *Talanta*, 2012, **99**, 897-903.  
9  
10 [23] G. Ma and L. Chen, *J. Chromatogr. A*, 2014, **1329**, 1-9.  
11  
12 [24] L. Chen and B. Li, *Food Chem.*, 2013, **141**, 23-28.  
13  
14 [25] C. Hu, J. Deng, Y. Zhao, L. Xia, K. Huang, S. Ju and N. Xiao, *Food Chem.*, 2014, **158**, 366-  
15 373.  
16  
17  
18 [26] D. He, X. Zhang, B. Gao, L. Wang, Q. Zhao, H. Chen, H. Wang and C. Zhao, *Food Control*,  
19 2014, **36**, 36-41.  
20  
21  
22 [27] F-F. Chen, X-Y. Xie and Y-P Shi, *J. Chromatogr. A*, 2013, **1300**, 112-118.  
23  
24 [28] X. Kong, R. Gao, X. He, L. Chen and Y. Zhang, *J. Chromatogr. A*, 2012, **1245**, 8-16.  
25  
26 [29] Y. Zhang, R. Liu, Y. Hu, and G. Li, *Anal. Chem.*, 2009, **81**, 967–976.  
27  
28  
29 [30] Y. Zhang, Y. Li, Y. Hu, G. Li and Y. Chen, *J. Chromatogr. A*, 2010, **1217**, 7337-7344.  
30  
31 [31] Y. Hu, Y. Li, R. Liu, W. Tan and G. Li, *Talanta*, 2011, **84**, 462-470.  
32  
33 [32] G.M. Lackmann, U. Salzberger, U. Tollner, M. Chen, S.G. Carmella and S.S. Hecht, *J. Natl.*  
34 *Cancer Inst.*, 1999, **91**, 459-465.  
35  
36 [33] S. Oga, Ateneu, São Paulo, 3rd edn., 2008.  
37  
38 [34] H. Kataoka, R. Inoue, K. Yagi and K. Saito, *J. Pharm. Biomed. Anal.*, 2009, **49**, 108-114.  
39  
40 [35] J.B. Patel, S.N. Shukla, H.R.H. Patel, K.K. Kothari, P.M. Shah and P.S. Patel, *Asian Pac. J.*  
41 *Cancer Prev.*, 2007, **8**, 229-235.  
42  
43 [36] S. Laurent, D. Forge, M. Port, A. Roch, C. Robic, L.V. Elst and R.N. Muller, *Chem. Rev.*,  
44 2008, **108**, 2064-2110.  
45  
46 [37] E. C. Figueiredo, D. M. de Oliveira, M. E. P. B. de Siqueira, M. A. Z. Arruda, *Anal. Chim.*  
47 *Acta*, 2009, **635**, 102-107.  
48  
49 [38] S. Kodama, A. Morikawa, K. Nakagomi, A. Yamamoto, A. Sato, K. Suzuki, T. Yamashita,  
50 T. Kemmei and A. Taga, *Electrophoresis* 2009, **30**, 349–356.  
51  
52  
53 [39] X. Shi, A. Wu, G. Qu, R. Li and D. Zhang, *Biomaterials*, 2007, **28**, 3741–3749.  
54  
55  
56  
57  
58  
59  
60

- 1  
2  
3  
4 [40] Guidance for Industry, Bioanalytical Method Validation, U.S. Department of Health and  
5 Human Services Food and Drug Administration, Center for Drug Evaluation and  
6 Research (CDER), Center for Veterinary Medicine (CVM), May 2001.  
7 <http://www.fda.gov/downloads/Drugs/Guidances/ucm070107.pdf>  
8  
9  
10 [41] C.N. Man, L-H. Gam, S. Ismail, R. Lajis and R. Awang, *J. Chromatogr. B*, 2006, **844**, 322-  
11 327.  
12  
13 [42] T. Tapani, J. Tom and R. Kari, *Clin. Chem.*, 1999, **45**, 2164-2172.  
14  
15  
16  
17  
18  
19  
20  
21  
22  
23  
24  
25  
26  
27  
28  
29  
30  
31  
32  
33  
34  
35  
36  
37  
38  
39  
40  
41  
42  
43  
44  
45  
46  
47  
48  
49  
50  
51  
52  
53  
54  
55  
56  
57  
58  
59  
60

**Table 1.**

Elemental composition of the materials obtained by EDS analyses.

Element	Fe <sub>3</sub> O <sub>4</sub>	Fe <sub>3</sub> O <sub>4</sub> @SiO <sub>2</sub>	Vinyl-modified Fe <sub>3</sub> O <sub>4</sub> @SiO <sub>2</sub>	MMIP
C	11.24	41.62	56.46	74.44
O	27.02	35.77	29.29	15.02
Si	-	10.60	6.27	4.02
Fe	54.02	4.79	3.54	2.40
Zn <sup>1</sup>	-	0.38	0.48	0.39
Cu <sup>2</sup>	0.72	0.86	0.49	0.42
Pt <sup>3</sup>	7.00	5.98	3.48	3.31
<b>Total</b>	<b>100.00</b>	<b>100.00</b>	<b>100.00</b>	<b>100.00</b>

<sup>1,2</sup>Impurities; <sup>3</sup>Platinum coating required to perform the SEM / EDS analyzes.**Table 2.**

Precision and accuracy for nicotine and cotinine extracted from urine by MMIP.

		Nicotine			Cotinine		
Intra-day	NC <sup>a</sup> /mg L <sup>-1</sup>	0.10	1.00	3.00	0.10	1.00	3.00
	OC <sup>b</sup> /mg L <sup>-1</sup>	0.10	1.02	3.15	0.09	1.06	3.16
	Precision <sup>c</sup> / %	7.85	7.47	9.68	19.63	4.81	14.20
	Accuracy <sup>d</sup> / %	4.09	1.90	4.93	-4.86	6.14	5.39
Inter-day	NC <sup>a</sup> /mg L <sup>-1</sup>	0.10	1.00	3.00	0.10	1.00	3.00
	OC <sup>b</sup> /mg L <sup>-1</sup>	0.11	0.94	2.77	0.10	0.91	2.88
	Precision <sup>c</sup> / %	12.55	10.01	13.45	8.62	14.28	8.41
	Accuracy <sup>d</sup> / %	7.85	-6.37	-7.74	2.71	-8.88	-3.97

<sup>a</sup> Nominal concentration; <sup>b</sup> obtained concentration; <sup>c</sup> as relative standard deviation, <sup>d</sup> as relative error.

## Captions for figures

1  
2  
3  
4  
5  
6  
7 **Fig. 1.** SEM images of  $\text{Fe}_3\text{O}_4$  (a),  $\text{Fe}_3\text{O}_4@\text{SiO}_2$  (b), vinyl-modified  $\text{Fe}_3\text{O}_4@\text{SiO}_2$  (c) and MMIP  
8 (d).  
9

10  
11 **Fig. 2.** AFM images: topography of  $\text{Fe}_3\text{O}_4$  (a) and  $\text{Fe}_3\text{O}_4@\text{SiO}_2$  (b); magnetic force microscopy  
12 (MFM) of  $\text{Fe}_3\text{O}_4$  (c) and  $\text{Fe}_3\text{O}_4@\text{SiO}_2$  (d).  
13  
14

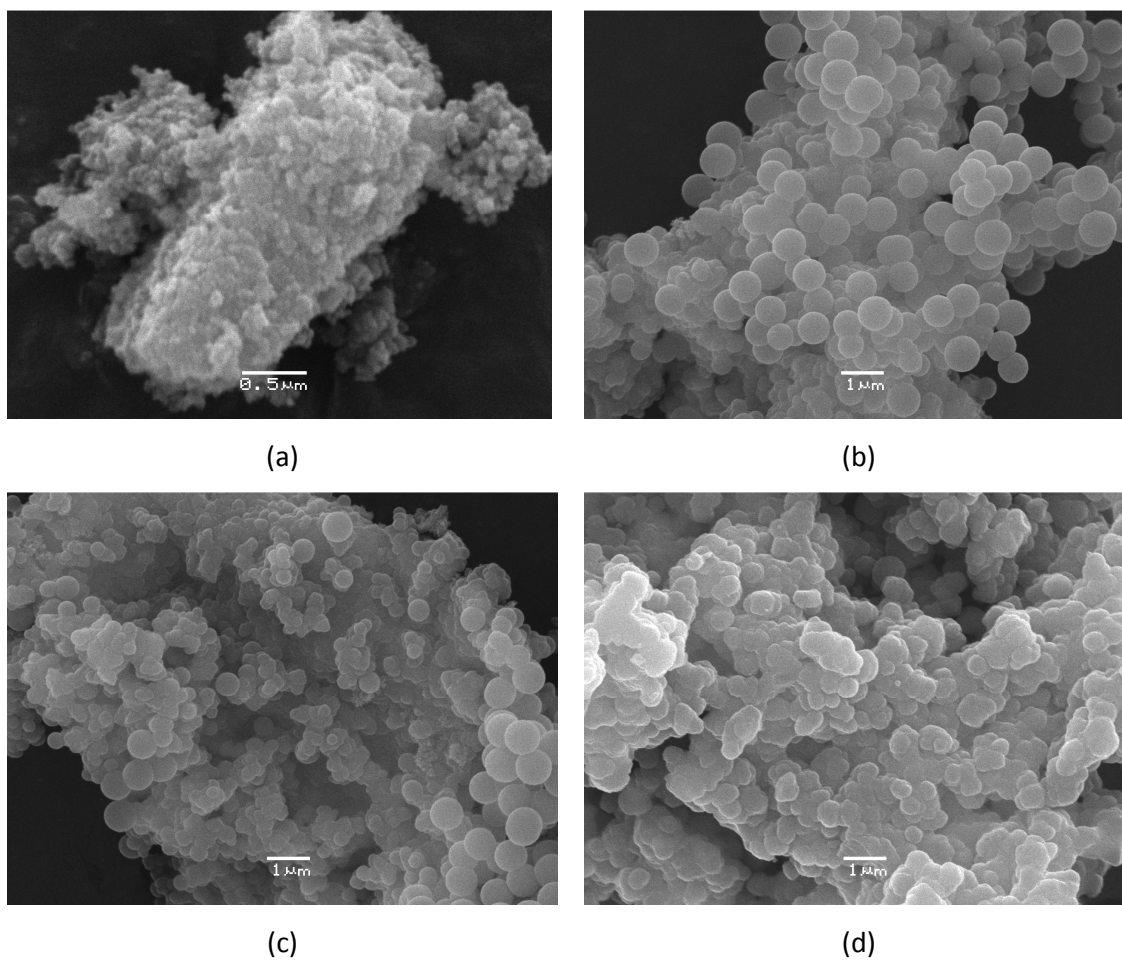
15 **Fig. 3.** FTIR spectra of  $\text{Fe}_3\text{O}_4$ ,  $\text{Fe}_3\text{O}_4@\text{SiO}_2$ , vinyl-modified  $\text{Fe}_3\text{O}_4@\text{SiO}_2$  and MMIP.  
16  
17

18 **Fig. 4.** TGA curves of  $\text{Fe}_3\text{O}_4$ ,  $\text{Fe}_3\text{O}_4@\text{SiO}_2$ , vinyl-modified  $\text{Fe}_3\text{O}_4@\text{SiO}_2$  and MMIP at a heating  
19 rate of  $10^\circ\text{C min}^{-1}$  from  $17^\circ\text{C}$  to  $800^\circ\text{C}$  in a nitrogen flow ( $100 \text{ mL min}^{-1}$ ).  
20  
21

22 **Fig. 5.** Mass spectra of nicotine and cotinine.  
23  
24

25 **Fig. 6.** Chromatogram of a urine sample from a non-smoker fortified with  $3.0 \text{ mg L}^{-1}$  of  
26 nicotine and cotinine.  
27  
28  
29  
30  
31  
32  
33  
34  
35  
36  
37  
38  
39  
40  
41  
42  
43  
44  
45  
46  
47  
48  
49  
50  
51  
52  
53  
54  
55  
56  
57  
58  
59  
60

Figure 1

1  
2  
3  
4  
5  
6  
7  
8  
9  
10  
11  
12  
13  
14  
15  
16  
17  
18  
19  
20  
21  
22  
23  
24  
25  
26  
27  
28  
29  
30  
31  
32  
33  
34  
35  
36  
37  
38  
39  
40  
41  
42  
43  
44  
45  
46  
47  
48  
49  
50  
51  
52  
53  
54  
55  
56  
57  
58  
59  
60

1  
2  
3  
4  
5  
6  
7  
8  
9  
10  
11  
12  
13  
14  
15  
16  
17  
18  
19  
20  
21  
22  
23  
24  
25  
26  
27  
28  
29  
30  
31  
32  
33  
34  
35  
36  
37  
38  
39  
40  
41  
42  
43  
44  
45  
46  
47  
48  
49  
50  
51  
52  
53  
54  
55  
56  
57  
58  
59  
60

Figure 2

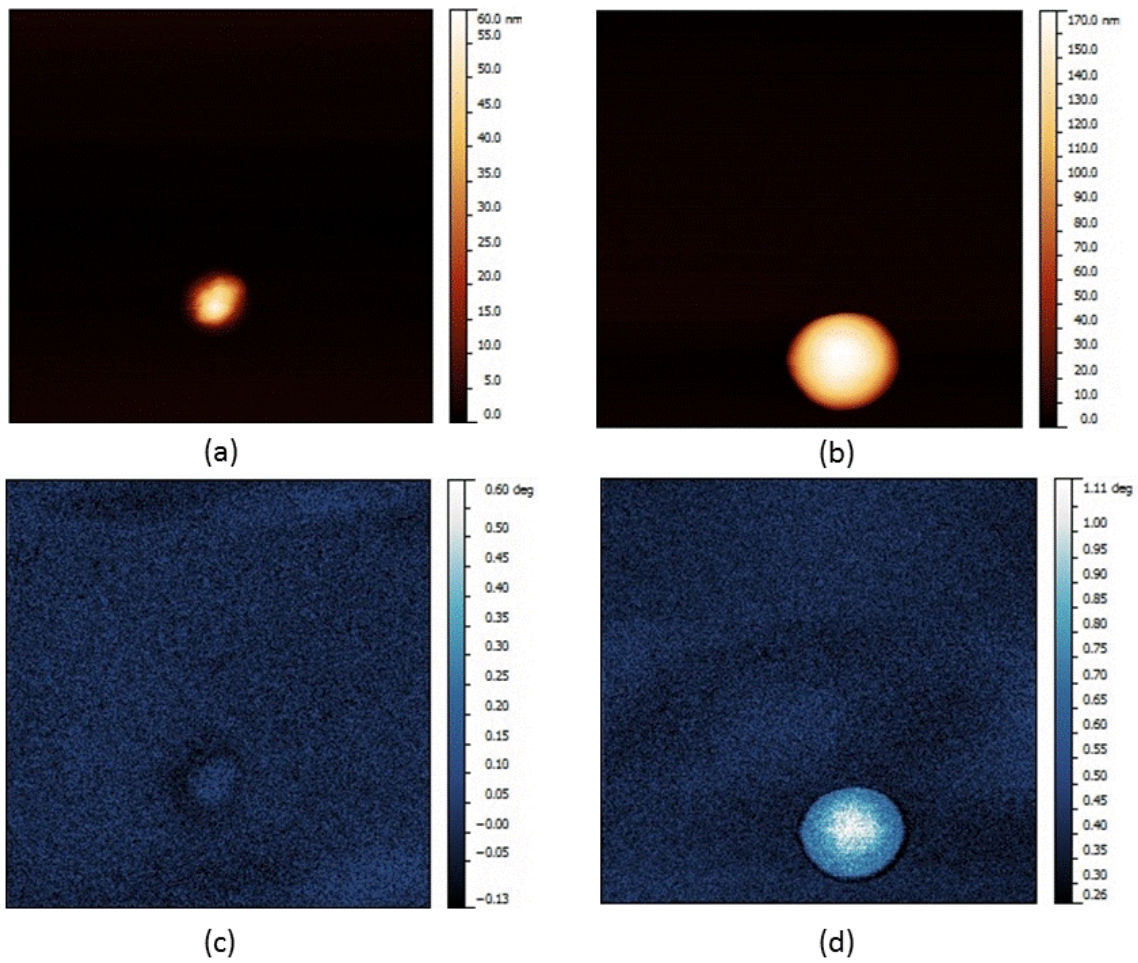
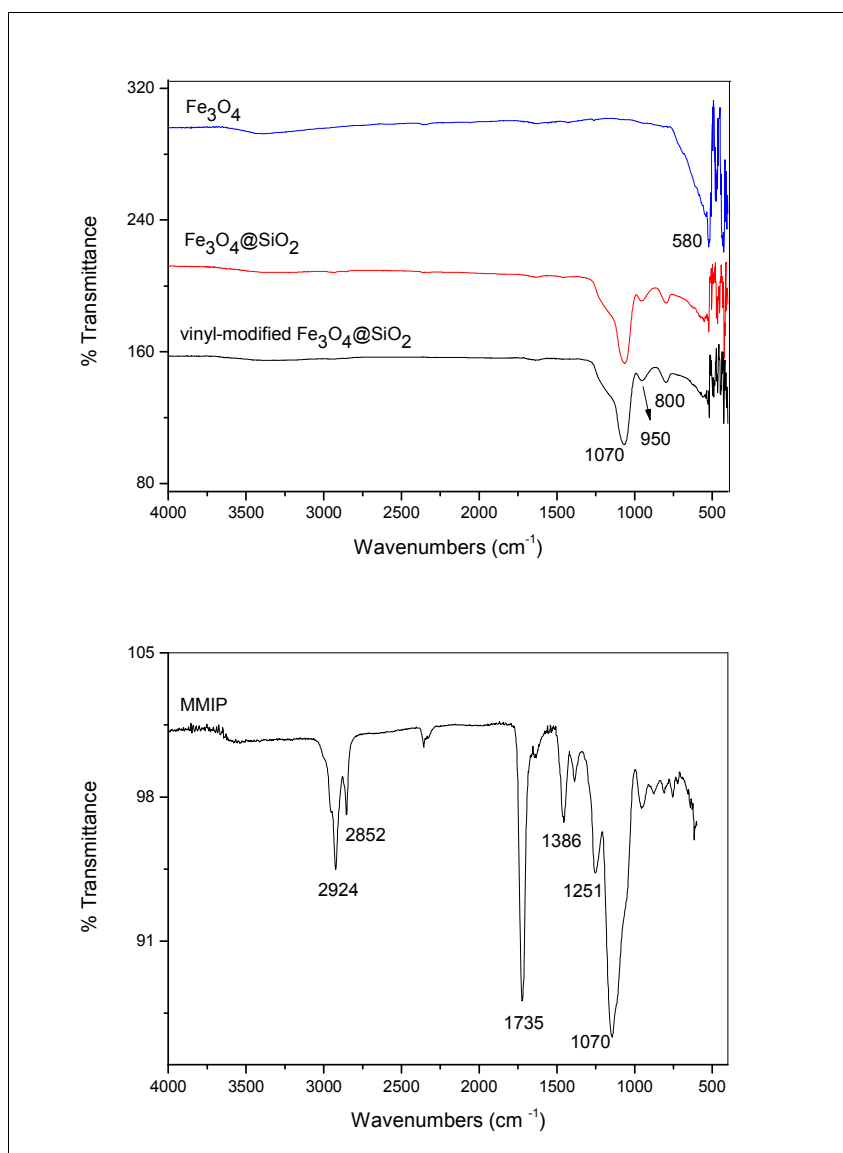


Figure 3

1  
2  
3  
4  
5  
6  
7  
8  
9  
10  
11  
12  
13  
14  
15  
16  
17  
18  
19  
20  
21  
22  
23  
24  
25  
26  
27  
28  
29  
30  
31  
32  
33  
34  
35  
36  
37  
38  
39  
40  
41  
42  
43  
44  
45  
46  
47  
48  
49  
50  
51  
52  
53  
54  
55  
56  
57  
58  
59  
60



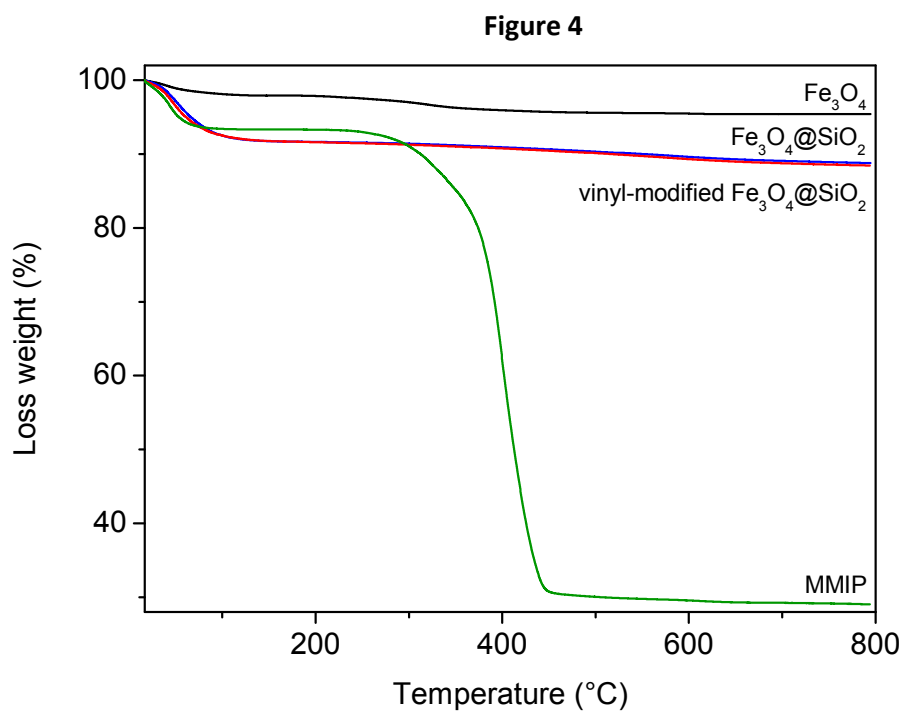
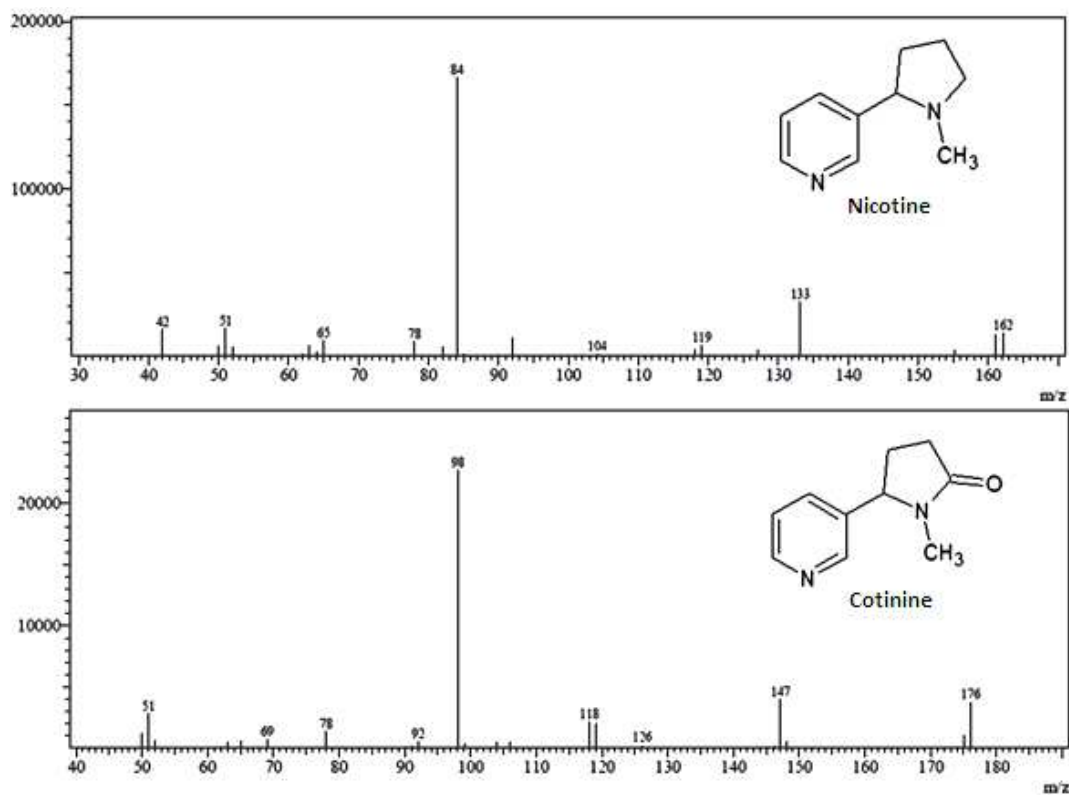




Figure 5

1  
2  
3  
4  
5  
6  
7  
8  
9  
10  
11  
12  
13  
14  
15  
16  
17  
18  
19  
20  
21  
22  
23  
24  
25  
26  
27  
28  
29  
30  
31  
32  
33  
34  
35  
36  
37  
38  
39  
40  
41  
42  
43  
44  
45  
46  
47  
48  
49  
50  
51  
52  
53  
54  
55  
56  
57  
58  
59  
60

1  
2  
3  
4  
5  
6  
7  
8  
9  
10  
11  
12  
13  
14  
15  
16  
17  
18  
19  
20  
21  
22  
23  
24  
25  
26  
27  
28  
29  
30  
31  
32  
33  
34  
35  
36  
37  
38  
39  
40  
41  
42  
43  
44  
45  
46  
47  
48  
49  
50  
51  
52  
53  
54  
55  
56  
57  
58  
59  
60

Figure 6

